MAGNETO-THERMOCAPILLARY-BUOYANCY CONVECTION IN A SQUARE CAVITY WITH PARTIALLY ACTIVE VERTICAL WALLS

by

Emtinene LAJNEF[a], Walid HASSEN[a], Lioua KOLSI[a,b*], Abdullah A. A. A. Al-RASHED[c], Rajab Al-SAYEGH[d], and Mohamed Naceur BORJINI[a]

[a] Research Unit for Metrology and Energy Systems, National Engineering Scholl of Monastire, University of Monastir, Monastir, Tunisia
[b] Mechanical Engineering Department, College of Engineering, Hail University, Hail City, Saudi Arabia
[c] Department of Automotive and Marine Engineering Technology, College of Technological Studies, The Public Authority for Applied Education and Training, Kuwait
[d] Department of Mechanical Engineering, College of Engineering, Northern Border University, Arar, Saudi Arabia

Original scientific paper
https://doi.org/10.2298/TSCI180126142L

Effect of magnetic field on combined surface tension and buoyancy convection in an enclosure with partially active vertical walls is investigated numerically. The active part of the left side wall is at a higher temperature than the active part of the right side wall. The bottom and the inactive parts of the side walls are adiabatic and capillary forces occur at the top free surface. The governing equations are discretized by the finite volume method. The results are obtained for $Pr = 0.054$, $0 \leq Ha \leq 100$, $0 \leq Ma \leq 10000$, *and* $2.10^4 \leq Gr \leq 2.10^6$. *The flow structure and temperature field were presented by streamlines and isotherms respectively. The surface tension effect of is manifested by increasing Marangoni number. The application of magnetic field was found to control the flow and to oppose the capillary effects.*

Key words: *Marangoni effect, natural convection, partially active walls, finite volume method*

Introduction

Thermocapillary or thermal Marangoni effect occurs when the transport phenomena along an interface under the effect of a surface tension gradient are caused by a temperature gradient. This phenomenon has a lot of interest both for its fundamental aspect and for its practical applications such as the process of crystalline growth, thermal insulation, nuclear reactors and solar collectors.

The thermocapillary convection problem has been the subject of several numerical and experimental studies. For 2-D problems, a recent numerical investigation based on a new FDM algorithm, which studies natural convection (MHD) in a differentially heated rectangular cavity, was carried out by Yu *et al.* [1]. Numerical simulations are performed in large ranges of Rayleigh and Hartmann numbers for a fixed Prandtl number ($Pr = 0.025$). The results show that

* Corresponding author, e-mail: lioua_enim@yahoo.fr

the application of the inclined magnetic field reduces the rate of heat transfer and can control of the flow.

Cen *et al.* [2] showed that the flow and temperature fields are considerably modified due to the Lorentz force. They proved that a vertical magnetic field magnitude equal to (128 mT) can dampen temperature fluctuations, particularly in the region near the growing crystal.

In addition, other remarkable and interesting works on the numerical modeling of crystal growth under natural convection were presented by James and Dubljevic [3], Grants and Gerbeth [4] and Satunkin [5].

Kandaswamy *et al.* [6] studied numerically the natural convection in a square cavity with partially heated vertical walls in the presence of a magnetic field. Based on the nine different combinations of active positions, they found that the rate of heat transfer is increased in thermally active (mid-middle) places while it is poor for the high-low case. They concluded that the mean Nusselt number increases with the increase of the Grashof number but decreases with the increase of the Hartmann number. Moreover, when Ha = 100, the convection is completely suppressed and the heat transfer in the cavity is mainly due to the conduction mode. A numerical study is carried out by Rudraiah *et al.* [7] to understand the effect of the magnetic field on the circulation caused by the combined buoyancy and thermocapillarity mechanism in an open rectangular cavity filled with a fluid of the low Prandtl number (Pr = 0.054). For large Marangoni number values, two counter-rotating cells are formed at the upper and lower half of the enclosure. They proved that if Hartmann number increases, the temperature field is similar to the conduction one and the current lines are elongated in the horizontal direction. The upper cell is crowded and stretched along the free surface. Hamimid and Amroune [8] studied the case of a laterally heated horizontal cavity with a shape ratio equal to 1 and Pr = 0.015 subjected to two forces of surface tension and buoyancy. The conclusions that can be drawn from this work are that in the case of the vertical magnetic field, the two isotherms and the current lines are equidistant. Also, the flow becomes unicellular and can be considered dominated by conduction phenomena.

On the other hand, in the case where the magnetic field is horizontal, the flow becomes multilayer since the intensity of the magnetic field increases and the maximum absolute values of the current function appear to be higher than the corresponding values obtained for the vertical field.

Hossain *et al.* [9] studied the thermocapillary convection problem combined with thermogravitational convection in a rectangular cavity for a liquid metal (Pr = 0.054). They studied the influence of variation of magnetic field direction and the presence of internal heat source on the flow and temperature fields. They represented the results for a Ma = 1000, the number of Grashof varying between $2\cdot10^4$ and $2\cdot10^6$, a Hartmann number between 0 and 40 and for a heat generation parameter, λ, between 0 and 40. The authors mentioned that a change in the direction of the external magnetic field from horizontal to vertical decreases the two thermo-gravitational convection cells while the surface tension forces increase the intensity of the thermocapillary cell.

They noticed that the increase in heat generation parameter increases the size of the gravitational convection cell until it occupies the entire cavity. Therefore it increases the forces of gravity by accelerating the flow of fluid. They further indicated that the fluid temperature increases when the internal heat generation parameter increases. Other interesting results related to MHD, thermo-capillary convection and partially heated cavity can be found in the literature [10-18].

To our knowledge the coupling between magnetic field, thermocapillary forces and buoyancy forces in a cavity equipped with partially heated walls has never been investigated. In the present work, we carry out a direct numerical study of magneto-thermocapillary-buoyancy convection in a partially active 2-D cavity.

Mathematical formulation and numerical method

Consider the unsteady 2-D natural convection flow of fluid in a square cavity of length, L, as shown in fig.1 filled with a fluid of low Prandtl number (Pr = = 0.054), the two side walls are partially and differentially heated. The other two horizontal walls are adiabatic. Gravity acts perpendicularly to the x-axis and the external magnetic field, B_0, is applied in parallel to gravity. The induced magnetic field is considered as negligible compared to the applied magnetic field. The free top surface is assumed to be flat and non-deformable. The surface tension at the upper limit is assumed to vary linearly with temperature. Under the above assumptions and under the Boussinesq approximation, the mass, motion and energy conservation equations in a 2-D Cartesian co-ordinate system are:

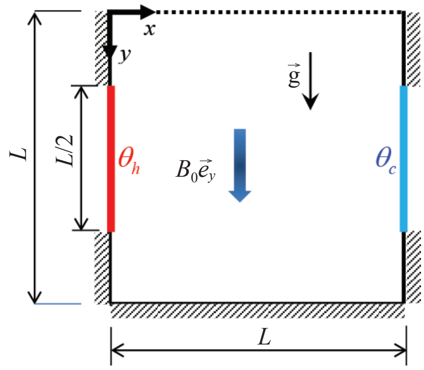

Figure 1. Physical geometry

$$\frac{\partial u}{\partial x}+\frac{\partial v}{\partial y}=0 \tag{1}$$

$$\frac{\partial u}{\partial t}+u\frac{\partial u}{\partial x}+v\frac{\partial u}{\partial y}=-\frac{1}{\rho}\frac{\partial p}{\partial x}+\nu\left(\frac{\partial^2 u}{\partial x^2}+\frac{\partial^2 u}{\partial y^2}\right)-\frac{\sigma_e B_0^2}{\rho}u \tag{2}$$

$$\frac{\partial v}{\partial t}+u\frac{\partial v}{\partial x}+v\frac{\partial v}{\partial y}=-\frac{1}{\rho}\frac{\partial p}{\partial y}+\nu\left(\frac{\partial^2 v}{\partial x^2}+\frac{\partial^2 v}{\partial y^2}\right)-\mathrm{g}\beta\left(\theta-\theta_c\right) \tag{3}$$

$$\frac{\partial \theta}{\partial t}+u\frac{\partial \theta}{\partial x}+v\frac{\partial \theta}{\partial y}=\alpha\left(\frac{\partial^2 \theta}{\partial x^2}+\frac{\partial^2 \theta}{\partial y^2}\right) \tag{4}$$

Based on the stream function-vorticity formalism and using the following dimensionless parameters:

$$X=\frac{x}{L},\quad Y=\frac{y}{L},\quad U=\frac{u}{\frac{\nu}{L}},\quad V=\frac{v}{\frac{\nu}{L}},\quad \tau=\frac{t}{\frac{L^2}{\nu}},\quad T=\frac{\theta-\theta_c}{\theta_h-\theta_c},\quad \Psi=\frac{\psi}{\nu},\quad \omega=\Omega\frac{L^2}{\nu}$$

The governing equations become:

$$U=-\frac{\partial \Psi}{\partial Y},\quad V=\frac{\partial \Psi}{\partial X} \tag{5}$$

$$\frac{\partial^2 \Psi}{\partial X^2}+\frac{\partial^2 \Psi}{\partial Y^2}=-\omega \tag{6}$$

$$\frac{\partial \omega}{\partial \tau}+U\frac{\partial \omega}{\partial X}+V\frac{\partial \omega}{\partial Y}=\frac{Gr}{2}\frac{\partial T}{\partial X}+\left(\frac{\partial^2 \omega}{\partial X^2}+\frac{\partial^2 \omega}{\partial Y^2}\right)-\mathrm{Ha}^2\frac{\partial U}{\partial Y} \tag{7}$$

$$\frac{\partial T}{\partial \tau}+U\frac{\partial T}{\partial X}+V\frac{\partial T}{\partial Y}=\frac{1}{\mathrm{Pr}}\left(\frac{\partial^2 T}{\partial X^2}+\frac{\partial^2 T}{\partial Y^2}\right) \tag{8}$$

where the non-dimensional parameters that appear in the equations are: $\mathrm{Pr}=\nu/\alpha$ Prandtl number, $\mathrm{Gr}=[g\beta(\theta_h-\theta_c)L^3]/\nu^2$ Grashof number, $\mathrm{Ha}=B_0L(\sigma_e/\mu)^{1/2}$ Hartmann number, and $\mathrm{Ma}=-(\partial\sigma/\partial\theta)\{[(\theta_h-\theta_c)L]/\mu\alpha\}$ Marangoni number. The local Nusselt number is defined by $\mathrm{Nu}=(1/2)(\partial T/\partial Y)$ resulting in the mean Nusselt number as $\overline{\mathrm{Nu}}=\int_0^1\mathrm{Nu}\,\mathrm{d}X$.

The boundary conditions are:

$$\psi=\frac{\partial\psi}{\partial X}=0 \quad \text{at} \quad X=0 \quad \text{and} \quad X=1$$

$$\psi=\frac{\partial\psi}{\partial Y}=0 \quad \text{at} \quad Y=1$$

$$\frac{\partial U}{\partial Y}=-\frac{1}{2}\frac{\mathrm{Ma}}{\mathrm{Pr}}\frac{\partial T}{\partial X} \quad \text{at} \quad Y=0$$

In active parts:

$$T=1 \quad \text{at} \quad X=1$$

$$T=0 \quad \text{at} \quad X=0$$

In inactive parts:

$$\frac{\partial T}{\partial X}=0 \quad \text{at} \quad X=1 \quad \text{and} \quad X=0$$

$$\frac{\partial T}{\partial Y}=0 \quad \text{at} \quad Y=1 \quad \text{and} \quad Y=0$$

The PDE (5)-(8) governing the MHD flow field with the associated boundary conditions has been written using FORTRAN language. All equations are integrated over a control volume with a central-difference scheme for treating convective terms. A fully implicit first order Euler time scheme is retained to discretize the temporal derivatives.

One obtains a set of algebraic equations for the vorticity, stream function and energy. This algebraic set of equations is solved using successive over relaxation (SOR) method based on the Gauss-Seidel iterative solver. Grid independency checks are performed and a uniform mesh with 101×101 control volumes is found sufficient enough for the desired accuracy. Finer meshes are tested showing no significant improvement in the results. The non-dimensional time step is chosen equal to 10^{-4} which ensures the stability of the calculations. The stopping criterion is satisfied as soon as:

$$\frac{\max\left|\psi^{k+1}-\psi^{k}\right|}{\max\left|\psi^{k}\right|}+\max\left|q^{k+1}-q^{k}\right|\leq 10^{-5}$$

for each time step, where the superscript *k* designates the k^{th} iteration of the SOR algorithm.

Results and discussion

The MHD-buoyancy-thermocapillay convection of an electrically conducting fluid is numerically investigated in a differentially heated square cavity with partially active walls. Nine configurations according to the positions of the active parts are studied. The numerical simulations are based on a wide range of parameters: Pr = 0.054, $0 \leq \text{Ha} \leq 100$, $0 \leq \text{Ma} \leq 10000$, and $2.10^4 \leq \text{Gr} \leq 2.10^6$. The flows caused by buoyancy and thermocapillary effects have strongly different origins. The buoyancy convection is due to density variation and thus its effect is distributed on the entire cavity, in opposition the thermocapillary effect which is a surface tension driven phenomenon occurs almost near of the free surface.

The chosen low value of Prandtl number corresponds to semi-conductor melts and liquid metals. The interaction between the magnetic field and the motion of such high electroconductivity fluids causes the creation of a Lorentz forces that affect the flow structure, temperature field and heat transfer rate that are presented respectively in terms of streamlines, isotherms and average Nusselt number. The main objective of the present work is to study the interaction and the mutual effects of magnetic, thermocapillary and buoyancy forces.

Code verification

Obtained Nusselt numbers for differentially heated square cavity for different Rayleigh number, Hartmann number, and Marangoni number are compared with those of Rudraiah *et al.* [7] and illustrated in tab. 1. It can be seen that our numerical results agree well with the earlier investigations, with maximum error around of 2 %.

Table 1. Code verification by results of Rudraiah *et al.* [7]

Gr	Ma	Ha	Nu [7]	Nu (present work)	Error [%]
20000	0	0	1.1144	1.1368	2.0082
	100	0	1.1163	1.0979	1.6466
		50	1.0164	1.0002	1.5930
		100	1.0062	1.0010	0.5128
	1000	0	1.4409	1.4137	1.8925
		50	1.1268	1.1094	1.5407
		100	1.0683	1.0449	2.1885
200000	0	0	1.9122	1.9528	2.1258
	100	0	1.9654	1.9902	1.2598
		50	1.0537	1.0466	0.6748
		100	1.0089	1.0053	0.3529
	1000	0	1.9795	1.9853	0.2925
		50	1.1391	1.1210	1.5916
		100	1.0671	1.0481	1.7833
	10000	0	2.7363	2.7741	1.3822
2000000	0	0	3.4048	3.4778	2.1449
	100	0	3.4848	3.5537	1.9783
		50	2.2504	2.3064	2.4898
		100	1.2686	1.2849	1.2793
	1000	0	3.6571	3.5824	2.0413
		50	2.3303	2.3223	0.3437
		100	1.3388	1.3241	1.0973
	10000	0	4.0971	4.0577	0.9614

Results without magnetic field

In absence of the vertical magnetic field, the flow structure and temperature fields inside the differentially heated square cavity with partially active walls are illustrated by the streamlines and isotherms in figs. 2 and 3 respectively. Figure 2 illustrates the competition between the termocapillary and buoyancy forces for Gr = 2.10^6, different values of Marangoni number and different active part locations. It should be noted that in the studied configuration, positive values of Marangoni number imply that thermocapillay and buoyancy forces are opposed since gravitational force and y-axis are downwards oriented. Thus buoyancy force tends to rotate the flow in clockwise direction and the opposite for the thermocapillay force. In absence of themocapillary effect, figs. 2(a)-2(c) the flow is characterized by one single clockwise cell with a perfect

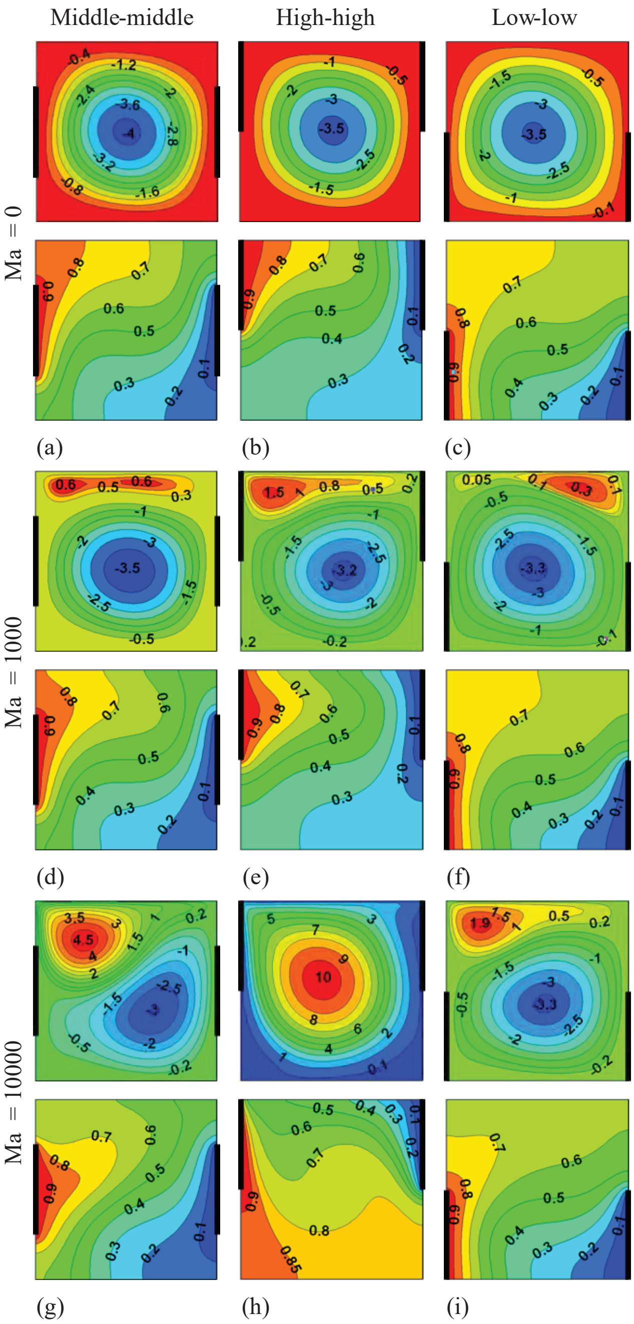

Figure 2. Stream function and isotherms contours for Ha = 0, Gr = 2.10^6 and different Marangoni number

central symmetry in the case *middle-middle* due to the symmetrical boundary conditions. Due thermocapillay force, the flow becomes divided into two regions; a top localized cell induced by the surface tension and a lower cell caused by the buoyancy force. For Ma = = 1000, the thermocapillay cell rotates anti-clockwise and grows stronger in size and intensity for the *high-high* case, fig. 2(e) due to the higher temperature gradient near of the free top surface. For higher Marangoni number (Ma = = 10000) the intensity of themocapillary induced flow is enhanced. For the *high-high* case, fig. 2(h). The flow structure is characterized by only one anti-clockwise cell. This is due to the increasing role played by the thermocapillary force that dominates the effect of gravitational force.

The temperature field is also affected by tension surface effects, which causes the distortion of isotherms at the center vertical line of the cavity. In addition isotherms become compacted near of the higher temperature active part especially for the *high-high*, case fig. 2(e).

Results with magnetic field

The interaction between the high conductive fluid motion and the magnetic field produces the Lorentz force that affects flow and temperature field in the cavity. The flow structure and the heat transfer is largely infected by the presence of thermocapillary forces, hence the need to control the flow by the application of the magnetic field.

The effect of the vertical magnetic field magnitude (Ha = 100) on the streamlines and isotherms is shown in fig. 3. In absence of thermocapillay effect and by applying the magnetic field the structure becomes bi-cellular with a strong reduction of the flow intensity especially at the core of the cavity, figs. 3(a)-3(c). By introducing the thermocapillary effect, the flow structure is affected especially for Ma = 10000. For all active part combinations cells are clockwise indicating that thermocapillary force is more sensitive to the magnetic field damping effect. This is expected, since the thermocapillary flow is mainly confined near the top free surface. This conclusion is boosted by the temperature field. In fact the magnetic field suppresses the central distortions, removes the vertical stratification and reduces the compaction near of the active walls. It is noted that the less distorted isotherms means a weak convective heat transfer.

Figure 4, presents the variations of average Nussselt number with Grashof number for the *middle-middle* case and different values of Hartmann number and Marangoni number. For low and moderate Marangoni number (0 and 1000) variations are increasing with Grashof number for all magnetic field strength. For higher Marangoni number (10000) variations presents a decreasing part for Gr < 2.10^5 due to the competitiveness between the thermocapillary and buoyancy forces. In this range of Grashof number the thermocapillary force dominates slightly and reduces the heat transfer rate by opposing the convective flow.

Note that magnetic forces greatly affect heat transfer and for Ha = = 100 the Nusselt number is almost constant and no longer depends on Grashof number.

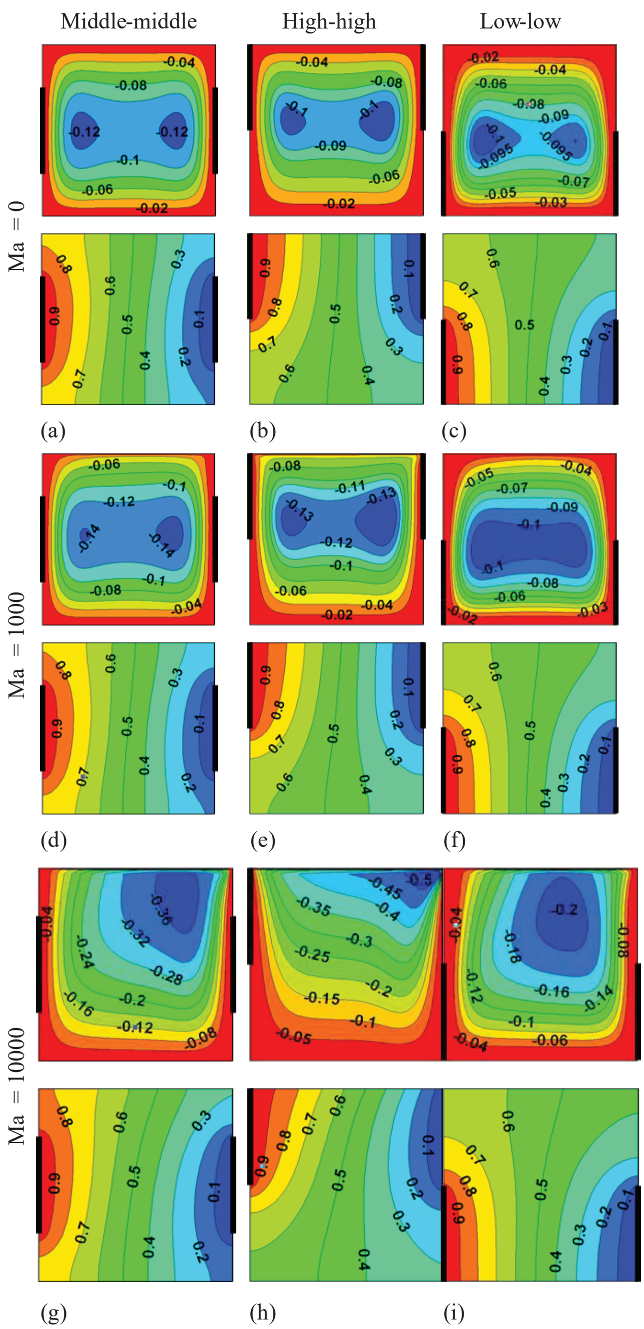

Figure 3. Stream function and isotherms contours for Ha = 100, Gr = 2.10^6 and different Marangoni number

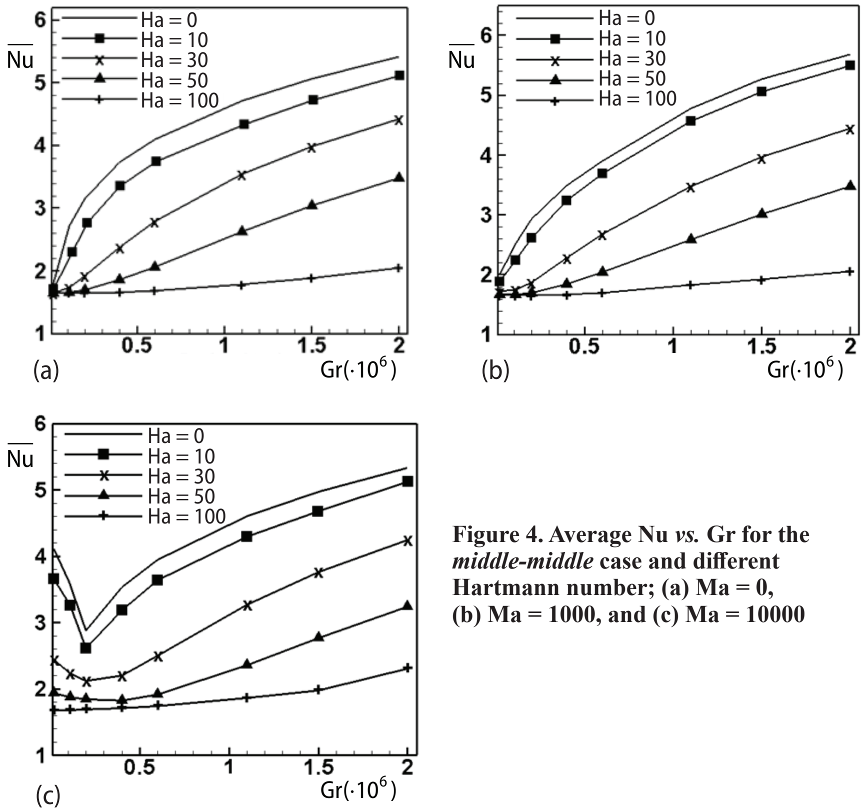

Figure 4. Average Nu *vs.* Gr for the *middle-middle* case and different Hartmann number; (a) Ma = 0, (b) Ma = 1000, and (c) Ma = 10000

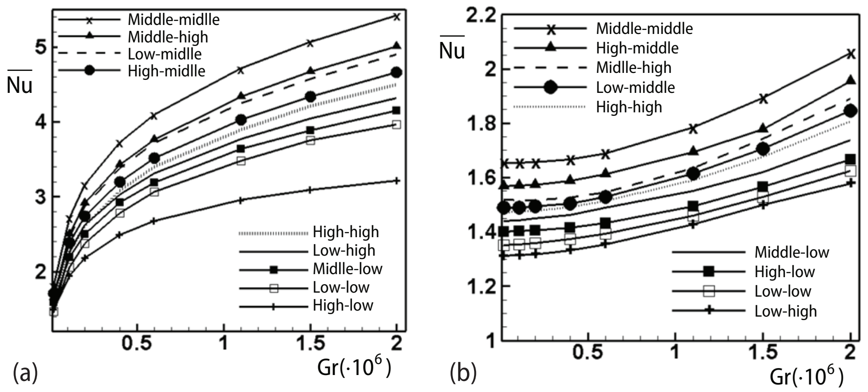

Figure 5. Average Nu *vs.* Gr for Ma = 1000; (a) Ha = 0, (b) Ha = 100

Figure 5 presents the variations of average Nusselt number *vs.* Grashof number for the nine studied case related to the position of the active parts. Results are presented in absence and in presence of the magnetic field for fixed Ma = 100. Results shows that the *middle-middle* case has higher heat transfer rate and *high-low* configuration presents the lower one. This is due to the positions of the active parts that are non-favourable for enhancing the convective flow (the higher part is at the top and the cold parts is at the bottom).

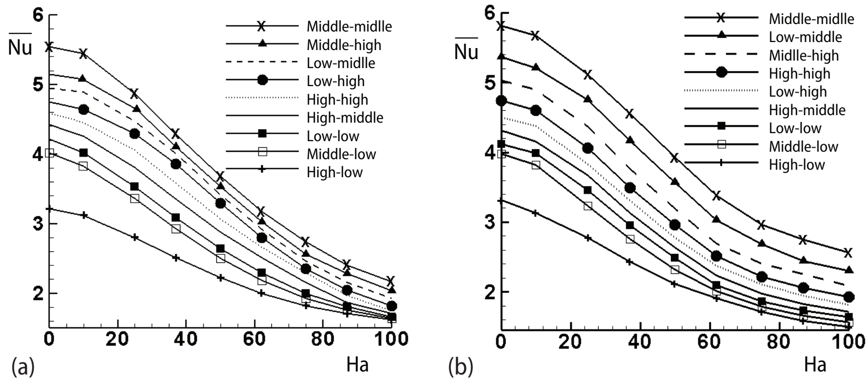

Figure 6. Average Nu *vs.* Hartman number for Gr = 2.10^6; (a) Ma = 0, (b) Ma = 10^4

The effect of the magnetic field on the heat transfer is presented in fig. 6, for the nine configurations and a fixed Grashof number, Gr = 2.10^6. With and without considering the thermocapillary effect the magnetic field is found to reduce the heat transfer especially for high Hartman numbers, this is due the produced Lorentz forces that oppose the convective flow. It is noticed that for all configurations and all Hartmann number, the average Nusselt is higher by considering the thermocapillary effect.

Conclusions

The effect of an external vertical magnetic field on the combined buoyancy and surface tension driven convection in partially differentially heated square cavity has been carried out numerically. The finite volume method is used to solve the governing equations for a wide range of dimensionless parameters and nine configurations related to the positions of the active parts are studied. The main findings of the study are presented as follows:

- The flow structure is affected by the thermocapillary force especially near of the free surface.
- For high magnetic field magnitude the temperature filed is similar to the pure conductive mode.
- The heat transfer rate is more important for the *middle-middle* case and is the lowest for the *top-bottom* case.
- For all Marangoni numbers (except for Gr < 2000, Ma > 10000 and Ha < 10), the average Nusselt number increases with Grashof number and decreases with Hartmann number.

Nomenclature

B_0 – magnetic field magnitude, [T]
Gr – Grashof number, [–]
g – gravitational acceleration, [ms^{-2}]
Ha – Hartmann number, [–]
L – enclosure width, [m]
Ma – Marangoni number, [–]
Nu – local Nusselt number, [–]
p – pressure, [Pa]
Pr – Prandtl number, [–]
Ra – Rayleigh number, [–]
T – dimensionless temperature, [–]
t – time, [s]
U, V – dimensionless velocities, [–]
X, Y – dimensionless Cartesian co-ordinates, [–]

Greek symbols

α – thermal diffusivity, [m^{2}s^{-1}]
β – thermal expansion coefficient, [K^{-1}]
θ – dimensionless variable of temperature, [–]
θ_c – cold temperature, [K]
θ_h – hot temperature, [K]
μ – dynamic viscosity, [kgm^{-1}s^{-1}]
ν – kinematic viscosity, [m^{2}s^{-1}]
ρ – density, [kgm^{-3}]
σ – surface tension, [Nm^{-1}]
ψ, Ψ – vector potential and dimensionless vector potential, [–]
Ω, ω – vorticity and dimensionless vorticity, [–]

References

[1] Yu, P. X., et al., Numerical Investigation of Natural Convection in a Rectangular Cavity under Different Directions of Uniform Magnetic Field, *International Journal of Heat and Mass Transfer, 67* (2013), Dec., pp. 1131-1144

[2] Cen, X., *et al*., Three Dimensional Simulation of Melt Flow in Czochralski Crystal Growth with Steady Magnetic Fields, *Journal of Crystal Growth, 340* (2017), 1, pp. 135-141

[3] James, N., Dubljevic, S., Optimal Boundary Control of a Diffusion-Convection-Reaction PDE Model with Time-Dependent Spatial Domain: Czochralski Crystal Growth Process, *Chemical Engineering Science, 67* (2012), 1, pp. 111-119

[4] Grants, I., Gerbeth, G., Rayleigh-Bernard Instability of Czochralski Configuration in a Transverse Magnetic Feld, *Journal of Crystal Growth, 358* (2012), Nov., pp. 43-50

[5] Satunkin, G., Modeling the Dynamics and Control Design for Czochralski, Liquid Encapsulated Czochralski and Floating Zone Processes, *Progress in Crystal Growth and Characterizations Materials, 56* (2010), 1-2, pp. 1-121

[6] Kandaswamy, P., *et al*., Magnetoconvection in an Enclosure with Partially Active Vertical Walls, *International Journal of Hheat and Mass Transfer, 51* (2008), 7-8, pp. 1946-1954

[7] Rudraiah, N., *et al*., Combined Surface Tension and Buoyancy-Driven Convection in a Rectangular Open Cavity in the Presence of a Magnetic Field, *Int. J. Non-Linear Mechanics, 30* (1995), 5, pp. 759-770

[8] Hamimid, S., Amroune, A., Marangoni-Natural Convection in Liquid Metals in the Presence of a Tilted Magnetic Field, *FDMP, 6* (2010), 4, pp. 369-384

[9] Hossain, M. A., *et al*., Buoyancy and Thermocapillary Driven Convection Flow of an Electrically Conducting Fluid in an Enclosure with Heat Generation, *International Journal of Thermal Sciences 44* (2005), 7, pp. 676-684

[10] Rahimi, A., *et al*., Experimental and Numerical Study on Heat Transfer Performance of Three-Dimensional Natural Convection in an Enclosure Filled with DWCNTs-Water Nanofluid- Experimental and Numerical Analysis, *Powder Technology, 322* (2017), Sept., pp. 340-352

[11] Salari, M., *et al*., 3D Numerical Analysis of Natural Convection and Entropy Generation within Tilted Rectangular Enclosures Filled with Stratified Fluids of MWCNTs/Water Nanofluid and Air, *Journal of the Taiwan Institute of Chemical Engineers, 80* (2017), Nov., pp. 624-638

[12] Kolsi, L., *et al*., Control of Natural Convection Via Inclined Plate of Cnt-Water Nanofluid in an Open Sided Cubical Enclosure under Magnetic Field, *International Journal of Heat and Mass Transfer, 111* (2017), Aug., pp. 1007-1018

[13] Kolsi, L., *et al*., Numerical Investigation of Combined Buoyancy-Thermocapillary Convection and Entropy Generation in 3D Cavity Filled with Al_2O_3 Nanofluid, *Alexandria Engineering Journal, 56* (2017), 1, pp. 71-79

[14] Maatki, C., *et al*., Inclination Effects of Magnetic Field Direction in 3D Double-Diffusive Natural Convection, *Applied Mathematics and Computation. 273* (2016), Jan., pp.178-189

[15] Mahian, O., *et al.,* Irreversibility Analysis of a Vertical Annulus Using TiO_2/Water Nanofluid with MHD Flow Effects, *International Journal of Heat and Mass Transfer, 64* (2013), Sept., pp. 671-679

[16] Mahian, O., *et al*., Entropy Generation between Two Vertical Cylinders in the Presence of MHD Flow Subjected to Constant Wall Temperature, *International Communications in Heat and Mass Transfer, 44* (2013), May, pp. 87-92

[17] Hayat, T., *et al*., Carbon Nanotubes Effects in the Stagnation Point Flow Towards a Nonlinear Stretching Sheet with Variable Thickness, *Advanced Powder Technology, 27* (2016), 4, pp. 1677-1688

[18] Hayat, T., *et al*., Nanofluid Flow through a Porous Space with Convective Conditions and Heterogeneous-Homogeneous Reactions, *Journal of the Taiwan Institute of Chemical Engineers, 70* (2017), Jan., pp. 119-126

Paper submitted: January 26, 2018
Paper revised: April 21, 2018
Paper accepted: April 24, 2018